Changes in the voltage profile of $Li/Li_{1+x}Mn_{2-x}O_4$ cells as a function of x

Yuan Gao
Department of Physics, Simon Fraser University, Burnaby, British Columbia, Canada V5A 1S6

J. N. Reimers
Moli Energy (1990) Limited, Maple Ridge, British Columbia, Canada V2X 9E7

J. R. Dahn
Department of Physics, Simon Fraser University, Burnaby, British Columbia, Canada V5A 1S6

(Received 10 January 1996)

$Li_{1+x}Mn_{2-x}O_4$ is a very promising candidate as the cathode material in state-of-the-art Li-ion rechargeable batteries. The ability to retain the initial capacity of the electrochemical cell upon cycling depends on the amount of the excess Li, represented as x in $Li_{1+x}Mn_{2-x}O_4$. Thus it is important to measure the voltage profiles of $Li/Li_{1+x}Mn_{2-x}O_4$ electrochemical cells carefully as a function of x. The twin peaks in the derivative curve, $-dy/dV$ versus V, where y denotes the amount of intercalated Li, are found to be weakened with increasing x. With a simple lattice-gas model, we show that the two peaks in the derivative curve are consistent with order-disorder phase transitions of Li ions, and the weakening of the peaks with increasing x is due to the presence of intercalated Li atoms pinned to the excess Li atoms which are substituted for Mn in the host lattice. [S0163-1829(96)06030-4]

INTRODUCTION

Lithium ion rechargeable batteries, which use lithium transition-metal oxides as the positive electrode and carbon as the negative electrode, not only have important applications in commerical electrons, but also are potential long-term candidates for powering emission-free vehicles.[1] Among the lithium transition-metal oxide intercalation compounds, $Li_{1+x}Mn_{2-x}O_4$ spinel has attracted a great deal of research[2] because of its economic and environmental advantages. It has been shown that adding excess lithium to the stoichiometric $LiMn_2O_4$ spinel helps maintain good cell capacity over a large number of cycles at the expense of the initial capacity.[3] The amount of excess lithium is represented by x in the notation $Li_{1+x}Mn_{2-x}O_4$ since the additional lithium atoms occupy the manganese sites (16*d* sites) in the spinel structure.[4,5]

It is well known[2,3,5,6] that the voltage profile of $LiMn_2O_4$ clearly exhibits a two plateau feature at about 4.0–4.1 V with a sharp voltage change of 0.15 V between the plateaus. This can also be seen in the derivative curve, $-dy/dV$ versus V, where y denotes the amount of intercalated lithium (as in $Li_{1+x-y}Mn_{2-x}O_4$), and in the cyclic voltammogram as two peaks with a valley between. These features are typical of order-disorder phase transitions.[7] Similar features due to order-disorder transitions have been observed in other lithium intercalation systems before. For example, the Li sites in $LiCoO_2$ can be divided into two sublattices. As lithium atoms are removed, they can either be removed from only one sublattice (ordered) or they can be removed randomly from both sublattices (disordered).[8] In Li_yCoO_2, Reimers and Dahn showed that the two peaks in the dy/dV of $Li/LiCoO_2$ cells at 4.05 and 4.17 V are due to order-disorder transitions, with the valley between signifying the ordering of Li ions on only one sublattice at half filling.[8] They also showed that the ordering of Li (and therefore the phase transition) is very sensitive to impurities and can be eliminated with only 2% Ni as the cation impurity in the system.[9] Therefore, it would be interesting to see how the two-peak feature in $Li_{1+x}Mn_{2-x}O_4$ changes with excess Li content x, considering that excess Li replaces Mn on the 16*d* sites, as the ''impurity'' among the 16*d* Mn atoms. It is also technologically important because the ability to retain the initial capacity in $Li/Li_{1+x}Mn_{2-x}O_4$ cells upon cycling depends on x as well.

Traditionally, the ordering of intercalated Li in a metal oxide framework can be treated with either a mean-field approach or with Monte Carlo simulations (both in the form of a lattice-gas model). These two approaches represent the two extremes, with the mean-field approximation best suited for systems with long-range interactions and the Monte Carlo method best suited for short-range interactions. Both methods have been observed to successfully model homogeneous systems without impurities,[10] in part because the short-range nature of the Li-Li interaction can be averaged out over a large number of atoms and modeled as a smaller long-range interaction.

In this paper, we will show how the voltage profile of $Li/Li_{1+x}Mn_{2-x}O_4$ electrochemical cells changes with excess Li, x, and then model the change using the lattice-gas model.

EXPERIMENT

All the samples were prepared by two consecutive heat treatments in air. First, Li_2CO_3 (FMC Corp.) and electrolytic manganese dioxide (EMD, Mitsui TAD 1 grade, 59.7% Mn by weight) were thoroughly mixed in a ratio corresponding to 1 Li per 2 Mn. About 70 g of this mixture was then heated to a first temperature, T_1, held for 18 h and then

TABLE I. Physical properties of the samples made in this study.

Sample	Nominal x	First heating temperature (°C)	Second heating temperature (°C)	a axis (Å)
$K1$	0.04	750	750	8.2442
$H9$	0.09	900	600	8.2318
$H11$	0.15	900	600	8.2069
$H12$	0.20	900	600	8.1923

cooled to room temperature in about 2 h. The heatings were made in an alumina boat placed within a horizontal tube furnace in air. Portions of the $LiMn_2O_4$ product were then mixed with an amount of additional Li salt calculated to give the desired final value of x in $Li_{1+x}Mn_{2-x}O_4$. This mixture was then heated in air to a second reaction temperature, T_2, soaked for 18 h and then cooled to room temperature at a rate of 50 °C/h. Table I shows the temperature conditions of the samples made.

Powder x-ray-diffraction measurements were made using a Siemens D5000 diffractometer equipped with a copper target x-ray tube and a diffracted-beam monochromator. All specimens were measured from 10° to 120° in scattering angle and each data collection took 15 h. There were no impurity peaks observed in any of the samples. The data was analyzed using Hill and Howard's[11] version of the Rietveld program. The lattice constants of the samples made here are included in Table I.

All electrochemical cells used 125 μm thick Li metal foil anodes and Celgard 2502 microporous polypropylene separators. Cathodes were made from the spinel powders, 5–10 % of Super S Carbon black (Chemetals Inc.) by weight and ethylene propylene diene terpolymer (EPDM) binder, uniformly coated on aluminum foil. The spinel powder and carbon black were added to a solution of 4% EPDM in cyclohexane such that 2% of the final electrode mass would be EPDM. Excess cyclohexane was then added until the slurry reached a suitable viscosity and then the slurry was spread on the aluminum foil with a film spreader. The cyclohexane was allowed to evaporate at room temperature in air. Electrodes were then compressed between flat plates at 120 bar pressure. Test electrodes were 1.2×1.2 cm squares with a typical thickness between 100 and 200 μm. The electrolyte used was 1 M $LiBF_4$ dissolved in a 50/50 volume mixture of ethylene carbonate and propylene carbonate (1 M $LiBF_4$ in EC/PC). Cell construction and sealing was carried out in an argon-filled glove box and 2325 coin-type hardware was used for the construction of cells. Details of the cell design can be found elsewhere.[12]

Cells were thermostatted at 30.0 ± 0.1 °C, then charged and discharged using constant current cyclers with $\pm1\%$ current stability. Charging and discharging correspond to deintercalating and intercalating of Li, respectively. Charge and discharge currents were ±7.40 mA/g of the $Li_{1+x}Mn_{2-x}O_4$ spinel cathode material. This corresponds to taking 20 h to remove all the lithium from $LiMn_2O_4$, since the theoretical capacity of $Li_{1+x}Mn_{2-x}O_4$ is about $(1-3x)$ 148 mA h/g.[3] Data were logged whenever the cell voltage changed by more than 0.002 V, or every 0.2 h, whichever occured first.

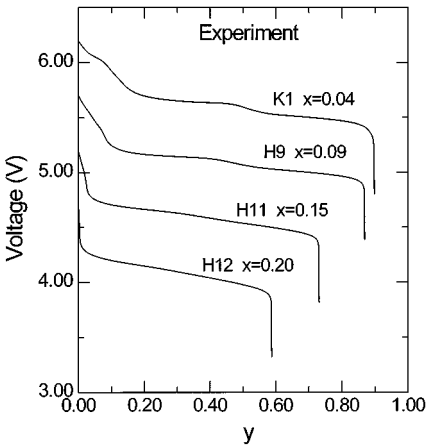

FIG. 1. The measured voltage curves for a series of samples with different x. The voltage curves of samples $H11$, $H9$, and $K1$ are sequentially shifted up to 0.5 V for clarity.

RESULTS AND DISCUSSION

The voltage profiles of the four samples are shown in Fig. 1 and their corresponding derivative curves, $-dy/dV$ versus V, are shown in Fig. 2, where y denotes the amount of intercalated lithium. As shown in Fig. 1, the kink in the voltage curve at about 4.1 V that could be due to a Li ordering transition is most pronounced in the curve with the smallest excess lithium content x. The kink becomes less visible as x increases, and the two-step character of the voltage profile is totally gone when $x=0.20$. This is more clearly seen in the derivative curves shown in Fig. 2, as the two peaks diminish with increasing x. This suggests that the presence of the additional lithium ions, that replace Mn on the 16d sites in the spinel structure, discourages the order-disorder phase transition by the Li ions on the 8a sites. This is possibly because some of the 8a Li ions are pinned by the additional 16d Li ions and this reduced freedom makes the ordering of the 8a Li more difficult.

Now that we have seen the effect of excess lithium on the

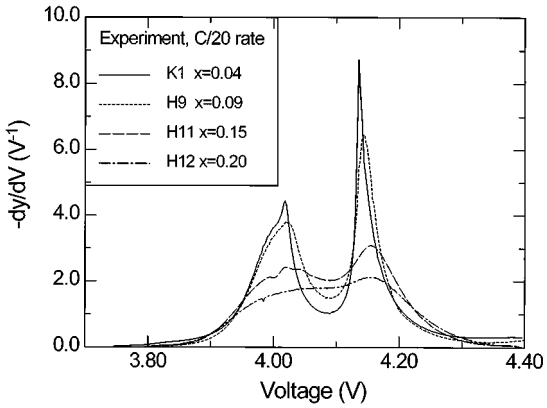

FIG. 2. The derivative curves, $-dy/dV$ versus V, obtained from the voltage curves in Fig. 1.

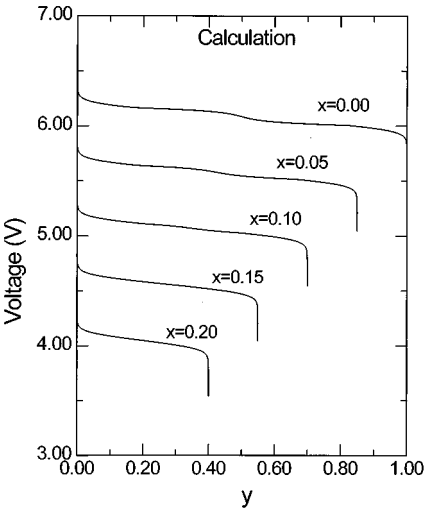

FIG. 3. The calculated voltage curves $V(y)$ for a series of values of x, assuming the $3x$ nonremovable Li are pinned. The voltage curves for $x=0.15$, 0.10, 0.05, and 0.00 are shifted up sequentially by 0.5 V for clarity.

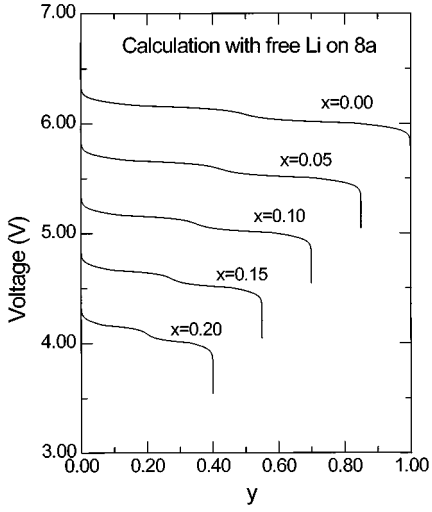

FIG. 4. The calculated voltage curves $V(y)$ for a series of values of x, assuming the $3x$ nonremovable Li are free to move around. The voltage curves for $x=0.15$, 0.10, 0.05, and 0.00 are shifted up sequentially by 0.5 V for clarity.

phase-transition feature in the voltage curve of $Li_{1+x}Mn_{2-x}O_4$, we will try to reproduce the feature using a simple lattice-gas model. In a lattice-gas model, the $8a$ Li ions are considered to be free to move on the $8a$ sublattice, while all other atoms are fixed. The interactions between an $8a$ Li and the host lattice result in a constant additive term to the voltage, and have no effect on the shape of the voltage curve. It is the $8a$ Li-$8a$ Li interactions that determine the shape of the voltage curve.

Modeling the $8a$ Li when $x=0$ (i.e., for $LiMn_2O_4$) is straightforward. The $8a$ sites in the spinel form a diamond lattice, which can be considered as two interpenetrating fcc sublattices separated by 1/4 1/4 1/4. Then, the Bragg-Williams approach is well suited for this system. Let y_1 and y_2 be the Li occupations on sublattice 1 and sublattice 2, respectively ($0\leqslant y_1,y_2\leqslant 1$). We will only consider the nearest and the second-nearest interactions between the Li ions. Since each Li atom has four nearest Li neighbors in the other sublattice and six second-nearest Li neighbors within the same sublattice, the Gibbs free energy of the lattice can be written as

$$G/N=E(y_1+y_2)+4J_1y_1y_2+3J_2y_1^2+3J_2y_2^2 - T(S_1+S_2)/N, \tag{1}$$

where N is the total number of sites in each sublattice, E is the site energy, J_1 and J_2 are the two-body interactions between the nearest Li neighbors and the second-nearest Li neighbors, respectively, T is the temperature, and

$$S_i=k\ \ln\left(\frac{N!}{(y_iN)![(1-y_i)N]!}\right) \tag{2}$$

is the configurational entropy of sublattice i. Noting that the chemical potential, $\mu=\partial(G/N)/\partial y_1=\partial(G/N)/\partial y_2$ at equilibrium, it can be shown that

$$y_i=[1+\exp(\varepsilon_i/kT)]^{-1}, \tag{3a}$$

where

$$\varepsilon_1=E-\mu+4J_1y_2+6J_2y_1 \tag{3b}$$

and

$$\varepsilon_2=E-\mu+4J_1y_1+6J_2y_2. \tag{3c}$$

Stirling's approximation $\ln N!\cong N\ \ln N-N$ was used. Equation (3) can be solved iteratively and the amount of intercalated Li, y, can be obtained from $y=(y_1+y_2)/2$ as a function of voltage V, noting that $\mu=-eV$.

Now we consider the case when $0<x<0.333$, i.e., for the general case of $Li_{1+x}Mn_{2-x}O_4$, where there is excess Li in the spinel. The amount of Li that can be taken out at practical voltages without altering the basic Mn-O framework is determined by the amount of Mn^{3+} ions.[3] Therefore, the removable Li is only $1-3x$ per formula unit of $Li_{1+x}Mn_{2-x}O_4$, since $Li_{1+x}Mn_{2-x}O_4$ can be written as $Li_{1+x}Mn^{III}_{1-3x}Mn^{IV}_{1+2x}O_4$.

First, we consider the case that the $3x$ nonremovable Li ions on $8a$ sites are ''pinned'' by the excess Li on the $16d$ sites. Let z_1 and z_2 be the occupations of the removable Li ions on sublatices 1 and 2, respectively ($0\leqslant z_1,z_2\leqslant 1$). The total Li occupations on the $8a$ sites can be expressed as

$$y_1=z_1(1-P_1)+1\cdot P_1 \tag{4a}$$

and

$$y_2=z_2(1-P_1)+1\cdot P_1 \tag{4b}$$

where P_1 is the probability of a particular $8a$ site being occupied by a fixed Li ion. Naturally, $P_1=3x$. Note that $3x\leqslant y_1,y_2\leqslant 1$ now. These changes obviously do not affect the form of Eq. (1), except that the entropy of sublattice i is now,

$$S_i=k\ \ln\left(\frac{N'!}{(z_iN')![(1-z_i)N']!}\right), \tag{5}$$

where $N'=(1-P_1)N$ is the total number of sites that removable Li can occupy.

Using the same relation $\mu=\partial(G/N)/\partial y_1=\partial(G/N)/\partial y_2$, now we have

$$z_i=[1+\exp(\varepsilon_i/kT)]^{-1}, \tag{6a}$$

where

$$\begin{aligned}\varepsilon_1&=E-\mu+4J_1y_2+6J_2y_1\\&=(E+12J_1x+18J_2x)-\mu+4J_1(1-3x)z_2\\&\quad+6J_2(1-3x)z_1,\end{aligned} \tag{6b}$$

and

$$\begin{aligned}\varepsilon_2&=E-\mu+4J_1y_1+6J_2y_2\\&=(E+12J_1x+18J_2x)-\mu+4J_1(1-3x)z_1\\&\quad+6J_2(1-3x)z_2.\end{aligned} \tag{6c}$$

Again Eq. (6) can be solved iteratively and the amount of the intercalated Li, y, can be obtained from $y=(z_1+z_2)(1-3x)/2$, as a function of voltage V. Note that Eqs. 3(a)–3(c) are now just a special case of Eqs. 6(a)–6(c) for $x=0$.

Figure 3 shows the calculated voltage curves using Eq. (6) for a series of calculations with different x. The values of the parameters used in Ref. 6 are as follows in order to give a close match to the measured voltage curve or derivative curve for the case of $x=0.00$:$E=-4.145$ eV, $J_1=37.5$ meV, and $J_2=-5$ meV. The temperature was 30 °C. It was found that a negative J_2 is necessary to strengthen the Li ordering and therefore the order-disorder transitions while simultaneously flattening the voltage profile. The calculated voltage curves agree with the experimental ones quite well, in that the kinks in the voltage curves are weakened with increasing x.

On the other hand, if the $3x$ nonremovable Li are not pinned, i.e., if they are free to move around, every site will be equivalent. Equations (4a) and (4b) are then

$$y_1=z_1(1-P_1)+z_1\cdot P_1=z_1 \tag{7a}$$

and

$$y_2=z_2(1-P_1)+z_2\cdot P_1=z_2. \tag{7b}$$

The amount of the intercalated Li will still be the same as expressed by $y=(z_1+z_2)(1-3x)/2$, because only $(1-3x)$ part of the total ''free'' Li population can be removed. Figure 4 shows the voltage curves calculated based on this senario. The experimental voltage curves are not modeled well, in that the kink is not weakened at all with increasing x. When the Li is free in the lattice, even with $3x$ nonremovable Li, there is no mechanism to weaken the Li ordering. Therefore, the totally free Li senario, even with $3x$ nonremovable Li, is wrong.

We propose that every 16d Li pins 3 other 8a Li ions near it. This is schematically shown in Fig. 5(a). The four Li ions taken together will have the same formal charge as a Mn^{4+} ion. Such clustering near the Li on 16d is expected. Li ions will be attracted because of the excess of negative charge on the oxygen atoms near the Li ion on 16d. There are six

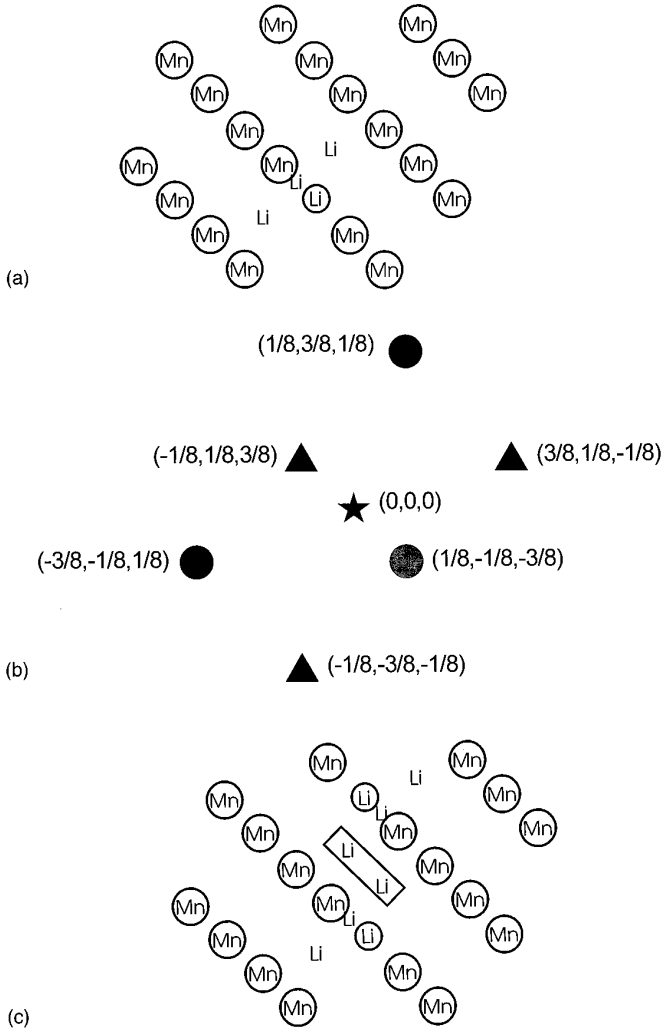

FIG. 5. (a) A schematic picture showing that one 16d Li pins three other 8a Li ions around it. The circled atoms are all in 16d sites. The three 8a Li ions are not in the same plane as the 16d Li and the other 16d Mn shown in the picture. (b) The six 8a sites that are the nearest to the 16d site. The star is the 16d site, the spheres are the 8a sites in the one fcc sublattice, and the triangles are the 8a sites in the other fcc sublattice. Their positions are labeled in the picture and the unit is the cubic lattice constant a. (c) A schematic picture showing one possible mechanism of pinning. The circled atoms are all in 16d sites. The noncircled Li are not in the same plane as the circled atoms. The boxed Li are in special sites pinned by both 16d Li atoms.

nearest 8a neighbors of each 16d site, with three in each fcc sublattice. Figure 5(b) shows their positions. When all the 16d Li are far apart, the 8a Li pinned nearby could cooperatively move onto either one set of three fcc sites or the other as needed to form the ordered state. However, when x is appreciable, some of the 8a Li sites will have more 16d Li atoms nearby. Such special sites are schematically shown in Fig. 5(c) and these will be most attractive for 8a Li. Since these special sites can randomly appear on either sublattice, the ordering will be frustrated. Our model calculation, which places 50% of the pinned Li on each sublattice, takes this into account.

Figure 6 shows the calculated derivative curve $-dy/dV$

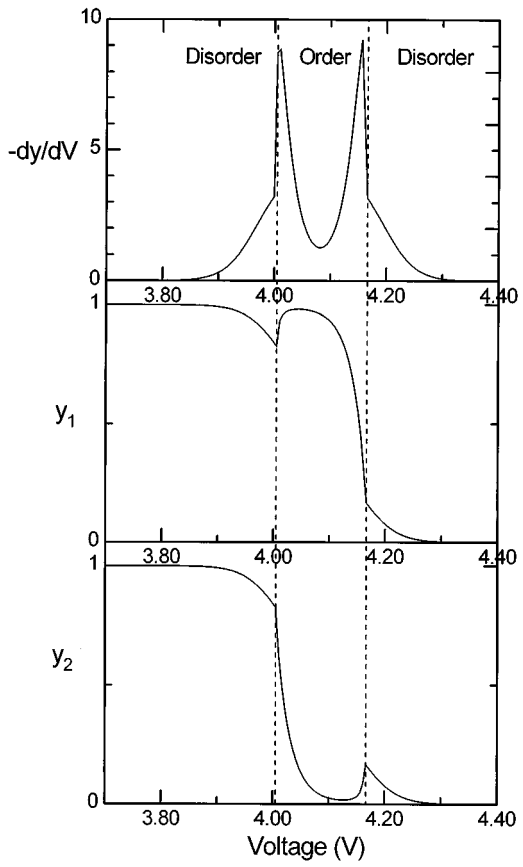

FIG. 6. The top panel shows the calculated derivative curve $-dy/dV$ for $x=0.00$, and the bottom two panels show the occupations of the two sublattices y_1 and y_2. They are all plotted versus the voltage. The two vertical dashed lines represent the boundaries between ordered and disordered phases.

for $x=0.00$ using Eq. (6), and the occupations of the two sublattices, y_1 and y_2, versus the voltage V. The two vertical dashed lines show the boundaries between ordered and disordered phases. As one goes from the right to the left (increasing the intercalated Li content), initially $y_1=y_2$ and Li are distributed randomly because there are not enough Li to form the ordered phase. At the first peak in $-dy/dV$, a disorder-to-order transition occurs, when the intercalated Li ions prefer to concentrate in one sublattice. This is called ordering. As the amount of the intercalated Li increases further and V is close to 4.0 V, this ordering is discouraged because there are not enough vacancies. Finally, an order-to-disorder phase transition occurs at the second peak in $-dy/dV$, and $y_1=y_2$ again.

Figure 7 shows the calculated derivative curves using Eq. (6). Comparing Fig. 7 with Fig. 2, one can claim success of the calculation in the following important aspect: The peaks due to order-disorder transitions get weakened, and eventually eliminated, with increasing x, which is also the case for the measured derivative curves. This suggests that the weakened order-disorder transitions are indeed due to the presence of the ''pinned'' Li in the $8a$ sublattice. If all of the $8a$ Li could move freely, the area under each derivative curve (the capacity) would be reduced, but the peaks in $-dy/dV$ would remain sharp as x increases.

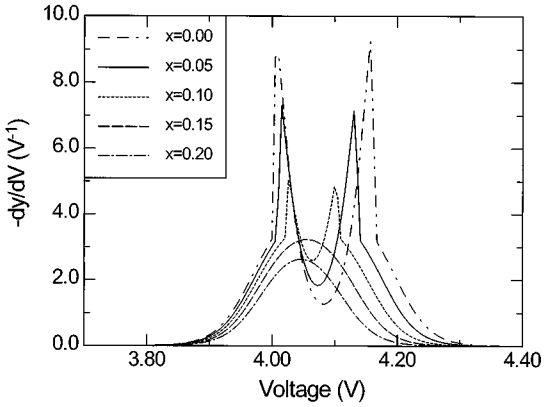

FIG. 7. The calculated derivative curves $-dy/dV$, for a series of x, using the mean-field approach, assuming $3x$ pinned Li atoms distributed equally on each sublattice.

Figures 2 and 7 show that the voltage distribution of the capacity becomes narrower with increasing x in the calculation, but stays more or less the same in the measurement. The discrepancy between the calculation and the measurement is easy to understand. As shown in Fig. 7, in addition to losing the phase-transition peaks, the capacity reduction with increasing x is at the expense of the part at the high voltage side. This is what is expected with the simple mean-field model described by Eqs. (4)–(6). In this model, the effect of the $3x$ pinned Li is felt throughout the lattice and by all other $8a$ Li atoms. The $3x$ pinned and the $(1-3x)$ removable Li are essentially the same in terms of the interactions between them. Thus, when materials with $x>0$ are ''empty'' (all removable Li gone) they still contain ''pinned'' Li. When free Li is added to these materials, it is as if the voltage profile begins at a point where the lattice is partly filled. Thus, the high voltage portion of the voltage profile is reduced. This, of course, does not reflect reality. As shown in Fig. 2, the voltage distribution of the capacity is not reduced as x increases. This suggests that the $3x$ pinned Li ions do not necessarily exhibit the same interactions as the $(1-3x)$ removable Li. For example, the free Li may try to stay away from the pinned Li at low concentrations due to short-range repulsive interactions. This would reduce the suppression of the high voltage capacity. However, the simple mean-field approach cannot deal with this, and more sophisticated calculations are necessary. Nevertheless, the most important feature, namely the change of the phase-transition peaks in the derivative curve, can be reproduced with a simple mean-field calculation, which assumes $3x$ $8a$ Li atoms are pinned near the Li atoms on the $16d$ sites.

In conclusion, we have carefully measured the voltage profiles of $Li_{1+x}Mn_{2-x}O_4$ as a function of x. The twin peaks in the derivative curve $-dy/dV$ versus V are found to be weakened with increasing x. With a simple mean-field solution to a lattice-gas model, it was shown that the two peaks in the derivative curve are consistent with order-disorder phase transitions of Li ions in the $8a$ sublattice. The weakening of the peaks with increasing x is due to the presence of

Li atoms in the $8a$ sublattice which are pinned near Li atoms on $16d$ sites as schematically shown in Fig. 5. If all the Li atoms on $8a$ sites are assumed to be mobile, and can rearrange as they like, then it is impossible to reproduce the changes in $-dy/dV$ and $V(y)$ which occur as x in $Li_{1+x}Mn_{2-x}O_4$ increases. We believe that these results shown that three Li atoms in $8a$ sites are pinned near each Li atom in $16d$ sites.

[1] See, for example, K. Brandt, Solid State Ionics **69**, 173 (1994); *Lithium Batteries, New Materials, Developments and Perspectives*, edited by G. Pistoia (Elsevier, New York, 1994).
[2] D. Guyomard and J. M. Tarascon, Solid State Ionics **69**, 222 (1994).
[3] R. J. Gummow, A. de Kock, and M. M. Thackeray, Solid State Ionics **69**, 59 (1994).
[4] R. G. Wyckoff, *Crystal Structures*, 2nd ed. (Krieger, Malabar, FL, 1981), Vol. 3.
[5] J. M. Tarascon, W. R. McKinnon, F. Coowar, T. N. Bowmer, G. Amatucci, and D. Guyomard, J. Electrochem. Soc. **141**, 1421 (1994).
[6] Yuan Gao and J. R. Dahn, J. Electrochem. Soc. **142**, 100 (1996).
[7] A. J. Berlinsky, W. G. Unruh, W. R. McKinnon, and R. R. Haering, Solid State Commun. **31**, 135 (1979).
[8] J. N. Reimers and J. R. Dahn, J. Electrochem. Soc. **139**, 2091 (1992).
[9] J. N. Reimers and J. R. Dahn, J. Electrochem. Soc. **140**, 2752 (1993).
[10] W. Li, J. N. Reimers, and J. R. Dahn, Phys. Rev. B **46**, 3236 (1992).
[11] R. J. Hill and C. J. Howard, J. Appl. Crystallogr. **18**, 173 (1985).
[12] A. M. Wilson and J. R. Dahn, J. Electrochem. Soc. **142**, 326 (1995).